Tyrosine phosphorylation of HuR by JAK3 triggers dissociation and degradation of HuR target mRNAs

Je-Hyun Yoon, Kotb Abdelmohsen*, Subramanya Srikantan, Rong Guo, Xiaoling Yang, Jennifer L. Martindale and Myriam Gorospe*

Laboratory of Genetics, National Institute on Aging-Intramural Research Program, NIH, Baltimore, MD 21224, USA

ABSTRACT

In response to stress conditions, many mammalian mRNAs accumulate in stress granules (SGs) together with numerous RNA-binding proteins that control mRNA turnover and translation. However, the signaling cascades that modulate the presence of ribonucleoprotein (RNP) complexes in SGs are poorly understood. Here, we investigated the localization of human antigen R (HuR), an mRNA-stabilizing RNA-binding protein, in SGs following exposure to the stress agent arsenite. Unexpectedly, the mobilization of HuR to SGs was prevented through the activation of Janus kinase 3 (JAK3) by the vitamin K3 analog menadione. JAK3 phosphorylated HuR at tyrosine 200, in turn inhibiting HuR localization in SGs, reducing HuR interaction with targets *SIRT1* and *VHL* mRNAs, and accelerating target mRNA decay. Our findings indicate that HuR is tyrosine-phosphorylated by JAK3, and link this modification to HuR subcytoplasmic localization and to the fate of HuR target mRNAs.

INTRODUCTION

Following transcription, RNA-binding proteins (RBPs) regulate post-transcriptional steps of gene expression, including pre-mRNA splicing, and mRNA transport, storage, stability and translation (1,2). Although some RBPs have general housekeeping functions on mRNAs [e.g. bind the mRNA 5′ cap or poly(A) tail], other specialized RBPs form ribonucleoprotein (RNP) interactions with discrete subsets of mRNAs which share specific sequence elements, and affect their post-transcriptional fate (3). The latter group includes RBPs such as human antigen R (HuR), AU-binding factor 1 (AUF1),

nucleolin and T-cell intracellular antigen (TIA)-1 and TIA-1-related (TIAR) proteins, which associate with subsets of target mRNAs and modulate their stability and/or translation rates (1,2). Specialized RBPs are directly involved in changing the patterns of expressed proteins in response to stress conditions, and such stress-response functions often require RBP post-translational modification (as reviewed in 4–6).

HuR has three RNA-recognition motifs (RRMs) through which it binds to a large collection of protein-coding and noncoding RNAs. Although it can interact with pre-mRNA intron sequences and has been linked to regulated splicing (7–9), HuR is best known for stabilizing and modulating the translation of mature mRNAs with which it associates via the 3′-untranslated region (UTR), typically at U-rich sites (9,10). Through binding to subsets of mRNAs encoding proliferative, stress-response and cell survival proteins, HuR has been implicated in cellular processes, such as cell division, survival, senescence and the stress-response, and with pathologies such as cancer (11,12).

HuR function is regulated at the levels of protein abundance, localization and post-translational modification. HuR levels are reduced by specific microRNAs (e.g. miR-519 and miR-125), by ubiquitination in response to mild heat shock and by caspase-mediated cleavage in response to severe stress (reviewed in 13). HuR is predominantly localized in the nucleus, but its effects on mRNA stability and translation are linked to its transport to the cytoplasm, which requires the HuR nucleocytoplasmic shuttling domain (HNS) and transport proteins such as transportins 1 and 2, the chromosome region maintenance 1 and importin-1α (14–17). The transport of HuR across the nuclear envelope is influenced by kinases including the cell cycle-dependent kinase (Cdk)1, AMP-activated protein kinase (AMPK), protein kinase (PK)C and the mitogen-activated protein kinase p38 (18–21). The interaction of HuR with target transcripts is modulated

through phosphorylation of serine and threonine residues by several kinases; phosphorylation by checkpoint kinase (Chk)2 generally reduced HuR interaction with mRNAs (22,23), whereas phosphorylation by activated p38 and PKC generally promoted HuR binding to mRNAs (4,24,25).

Besides altering the ratio of cytoplasmic-to-nuclear HuR and the interaction of HuR with target mRNAs, a number of stress agents (e.g. heat shock, irradiation with ultraviolet light and treatment with hydrogen peroxide) can also enhance the aggregation of HuR in cytoplasmic RNP foci named stress granules (SGs) (14,26–29). SGs assemble in response to cell-damaging conditions to halt the translation of housekeeping mRNAs and to selectively allow stress-response and repair proteins to be translated (30). Besides HuR, SGs also contain numerous other RBPs, such as poly(A)-binding protein (PABP), staufen, tristetraprolin, TIA-1, TIAR, RasGAP-associated endoribonuclease (G3BP), fragile X mental retardation syndrome, survival of motor neuron and cytoplasmic polyadenylation element binding proteins (30). SGs are dynamic RNP structures that assemble rapidly when the cell encounters stress and disassemble in a timely manner after the stress discontinues. SGs are believed to be the sites of mRNA 'triage' where decisions are made on the stability of individual mRNAs while the global cellular translation is halted.

Despite the key role of HuR in the cellular stress-response, the mechanisms that control HuR localization in SGs and their possible impact on expression of HuR target stress-response mRNAs are unknown. Here, we report that in human cervical carcinoma cells, the arsenite-triggered accumulation of HuR in SGs is accompanied by increased HuR binding to target transcripts *SIRT1* and *VHL* mRNAs and by stabilization of these mRNAs. Unexpectedly, the accumulation of HuR in SGs was blocked by treatment with menadione, a drug that activated the tyrosine kinase Janus kinase 3 (JAK3). JAK3 phosphorylated three HuR tyrosine residues *in vitro*; mutagenesis to prevent HuR phosphorylation specifically at Y200 restored HuR accumulation in SGs, preserved HuR binding to *SIRT1* and *VHL* mRNAs and rescued their stability. These studies link HuR presence in SGs with the fate of target mRNAs, and highlight a novel function of tyrosine kinase JAK3 as regulator of HuR function.

MATERIALS AND METHODS

Cell culture, chemicals, transfection, small interfering RNAs and plasmids

Human HeLa cells were cultured in Dulbecco's modified Eagle's medium (Invitrogen) supplemented with 10% (v/v) Fetal Bovine Serum (FBS) and antibiotics. All plasmids were transfected using Lipofectamine-2000 (Invitrogen) and analyzed 48 h later. JAK3 and Chk2 siRNAs were from Santa Cruz Biotechnology. For mRNA stability assays, HeLa cells were treated with actinomycin D (2.5 µg/ml) to inhibit *de novo* transcription. Actinomycin D, arsenite (sodium arsenite) and menadione were from

Sigma; pateamine A (used at 50 nM) was a gift from I.E. Gallouzi. A site-directed mutagenesis kit (Stratagene) was used to introduce point mutations in HuR expression vectors.

Western blot analysis

Whole-cell lysates, prepared in Radioimmunoprecipitation assay (RIPA) buffer, were separated by sodium dodecyl sulphate-polyacrylamide gel electrophoresis, and transferred onto Polyvinylidene fluoride (PVDF) membranes (Invitrogen iBlot Stack). Primary antibodies recognizing HuR, PABP, TIA-1, JAK3, p(Y980)JAK3, p(T68)Chk2, Chk2, Tubulin, eIF2α and phosphorylated (p-)eIF2α were from Santa Cruz Biotechnology. Antibodies recognizing phosphotyrosine (pY) residues and Flag were from Cell Signaling and Sigma, respectively. HRP-conjugated secondary antibodies were from GE Healthcare.

Immunoprecipitation assays

For immunoprecipitation (IP) of endogenous RNP complexes from whole-cell extracts (22), cells were lysed in 20 mM Tris-HCl at pH 7.5, 100 mM KCl, 5 mM $MgCl_2$ and 0.5% NP-40 for 10 min on ice and centrifuged at 10 000 g for 15 min at 4°C. The supernatants were incubated with protein A-Sepharose beads coated with antibodies that recognized HuR, Jak3 or Flag or with control IgG (Santa Cruz Biotechnology) for 1 h at 4°C. After the beads were washed with NT2 buffer (50 mM Tris-HCl at pH 7.5, 150 mM NaCl, 1 mM $MgCl_2$ and 0.05% NP-40), the complexes were incubated with 20 U of RNase-free DNase I (15 min at 37°C) and further incubated with 0.1% sodium dodecyl sulphate/0.5 mg/ml proteinase K (15 min at 55°C) to remove DNA and proteins, respectively. The RNPs isolated from the IP materials were further assessed by reverse transcription (RT) using random hexamers and Maxima Reverse Transcriptase (Thermo Scientific) and real-time, quantitative (q) polymerase chain reaction (PCR) using gene-specific primers (Supplementary Table S1) as well as by western blot (WB) analysis.

RNA analysis

Trizol (Invitrogen) was used to extract total RNA, and acidic phenol (Ambion) was used to extract RNA for RIP analysis (22). RT-qPCR analysis was performed using gene-specific primers (Supplementary Table S1) and SYBR green master mix (Kapa Biosystems), in an Applied Biosystems 7300 instrument. For polyribosome distribution analysis, cells were treated with cycloheximide (100 µg/ml, 15 min), and the resulting lysates (500 µl) were separated by ultracentrifugation through 10–50% linear sucrose gradients. The relative absorbance at UV 254 nm was recorded to trace the amount of RNAs throughout the gradients.

Biotin pulldown analysis

Recombinant maltose-binding protein (MBP)-HuR was incubated with a buffer containing 20 mM Tris-HCl at

pH 7.5, 100 mM KCl, 5 mM MgCl$_2$ and 0.5% NP-40. Biotinylated *SIRT1* and *GAPDH* 3′-untranslated regions were synthesized by PCR amplification of cDNA using forward primers that contained the T7 RNA polymerase promoter sequence (Supplementary Table S1) in the presence of biotinylated CTP and T7 RNA polymerase, as described (22,31). Proteins present in the pulldown material were studied by WB analysis.

In vitro kinase assay

To analyze the phosphorylation of HuR *in vitro*, MBP-HuR purified from *Escherichia coli* was incubated with JAK3 protein immunoprecipitated from HeLa cells or purchased from Millipore. The assay was performed in kinase reaction buffer as described previously (31).

Liquid chromatography-tandem mass spectrometry analysis

Protein samples were processed using the 'Filter-Assisted Sample Preparation' (FASP) method (32). Briefly, protein samples were dissolved in urea (9 M) and subjected to reduction [5 mM Tris-(2-Carboxyethyl)phosphine, hydrochloride (TCEP), Sigma] at 60°C for 45 min and to alkylation (20 mM C$_2$H$_4$INO, Sigma) at 25°C for 15 min. Protein samples were cleaned using a 30-kDa Amicon Filter (UFC503096, Millipore) with urea (9 M) and NH$_4$HCO$_3$ (30 mM). Samples were then proteolyzed with trypsin (Promega) and chymotrypsin (Roche) for 12 h at 37°C (1: 20 ratio). The digested peptides were desalted and eluted with 0.1% trifluoroacetic acid in 60% acetonitrile. Dry extracted peptides were resuspended in 7 μl 0.1% formic acid for Liquid chromatography-tandem mass spectrometry (LC–MS/MS) analysis. Tandem mass spectrometry analysis of the peptides was conducted on LTQ-Orbitrap Velos interfaced with a 2D nanoLC system nanoACQUITY UltraPerformance LC System. Precursor and fragment ions were analyzed at 30 000 and 7500 resolutions, respectively. Peptide sequences were identified from isotopically resolved masses in MS and MS/MS spectra extracted with and without deconvolution using Thermo Scientific Xtract software. The data were analyzed using Proteome Discoverer 1.3 (Thermo Scientific) software configured with Mascot and Sequest search nodes and searched against Refseq version 46, human entries with oxidation on methionine, deamidation on residues N and Q, phosphorylation of Ser/Thr/Tyr residues as different variable modifications and carbamidomethyl group on cysteine residue as fixed modification. Mass tolerances on precursor and fragment masses were set to 15 ppm and 0.03 Da, respectively. Peptide validator node was used for peptide confirmation, and a 1% false discovery rate cutoff was used to filter the data.

Immunofluorescence assay

Cells were fixed with 2% (v/v) formaldehyde, permeabilized with 0.2% (v/v) Triton X-100, blocked with 5% (w/v) bovine serum albumin and incubated with primary antibodies recognizing HuR (Santa Cruz Biotechnology), TIA-1 (Santa Cruz Biotechnology), eIF3b (Santa Cruz Biotechnology), G3BP (BD biosciences) or Flag (Sigma).

Alexa 488- or Alexa 568-conjugated secondary antibodies (Invitrogen) were used to detect primary antibody-antigen complexes with different color combinations as needed. Images were acquired using Axio Observer microscope (ZEISS) with AxioVision 4.7 Zeiss image-processing software or with LSM 510 Meta (ZEISS).

RESULTS

JAK3 phosphorylates HuR and prevents its accumulation in SGs

HuR is normally a nuclear protein, as seen in HeLa cells (Figure 1A, control), but it can translocate to the cytoplasm on stress. In response to specific stress conditions, such as arsenite treatment, HuR was further mobilized to cytoplasmic SGs (Figure 1A). While performing experiments to test the presence of HuR in SGs after stress, we made the serendipitous discovery that 15 μM menadione (a chemotherapeutic agent that causes oxidative damage) enhanced HuR presence in the cytoplasm, but did not trigger HuR-positive SGs. Unexpectedly, menadione also prevented SG formation following exposure to 250 μM arsenite (Figure 1A, Supplementary Figure S1A). The combined treatment with arsenite and menadione caused oxidative damage, as assessed by monitoring fluorescence after incubation with dihydrocalcein, an indicator of reactive oxygen species (Supplementary Figure S1B). Although treatment with arsenite and menadione did not elicit immediate signs of apoptotic cell death by 4 h after treatment (Supplementary Figure S1C and D), some cell loss and evidence of apoptosis were detectable by 24 h following treatment (Supplementary Figure S1C and D). The formation of SGs appeared to be generally suppressed under these conditions, as other markers used to visualize SGs [e.g. G3BP and TIA-1 (Figure 1B)] similarly failed to aggregate in SGs. However, we could not exclude the possibility that SGs might have been visualized by testing for other SG markers, that SG formation was delayed or that SGs were too small for detection. Arsenite treatment blocked translation globally (33); however, despite impairing SG formation, menadione did not rescue the translationally inhibited state, as evidenced by the fact that polysomes remained globally suppressed, eIF2α was still phosphorylated and HuR remained bound to PABP (Supplementary Figure S2). To test whether menadione prevented the recruitment of HuR to SGs that formed in an eIF2α-dependent or -independent manner, we studied the effect of 50 nM pateamine A, a drug that induces SG formation independently of eIF2α phosphorylation (34). As shown (Figure 1C), pateamine A-triggered SGs were not blocked by menadione treatment, suggesting that menadione blocked the recruitment of HuR to SGs triggered by eIF2α phosphorylation.

To investigate the mechanisms underlying the dynamics of HuR assembly in SGs, we screened a library of kinase inhibitors (described in 35) for restoration of HuR-positive SGs. Among the compounds in the library, only the JAK3 inhibitor ZM 449829 was capable of reversing the effect of menadione and restoring SGs in cells treated concomitantly with arsenite and menadione (Figure 2A
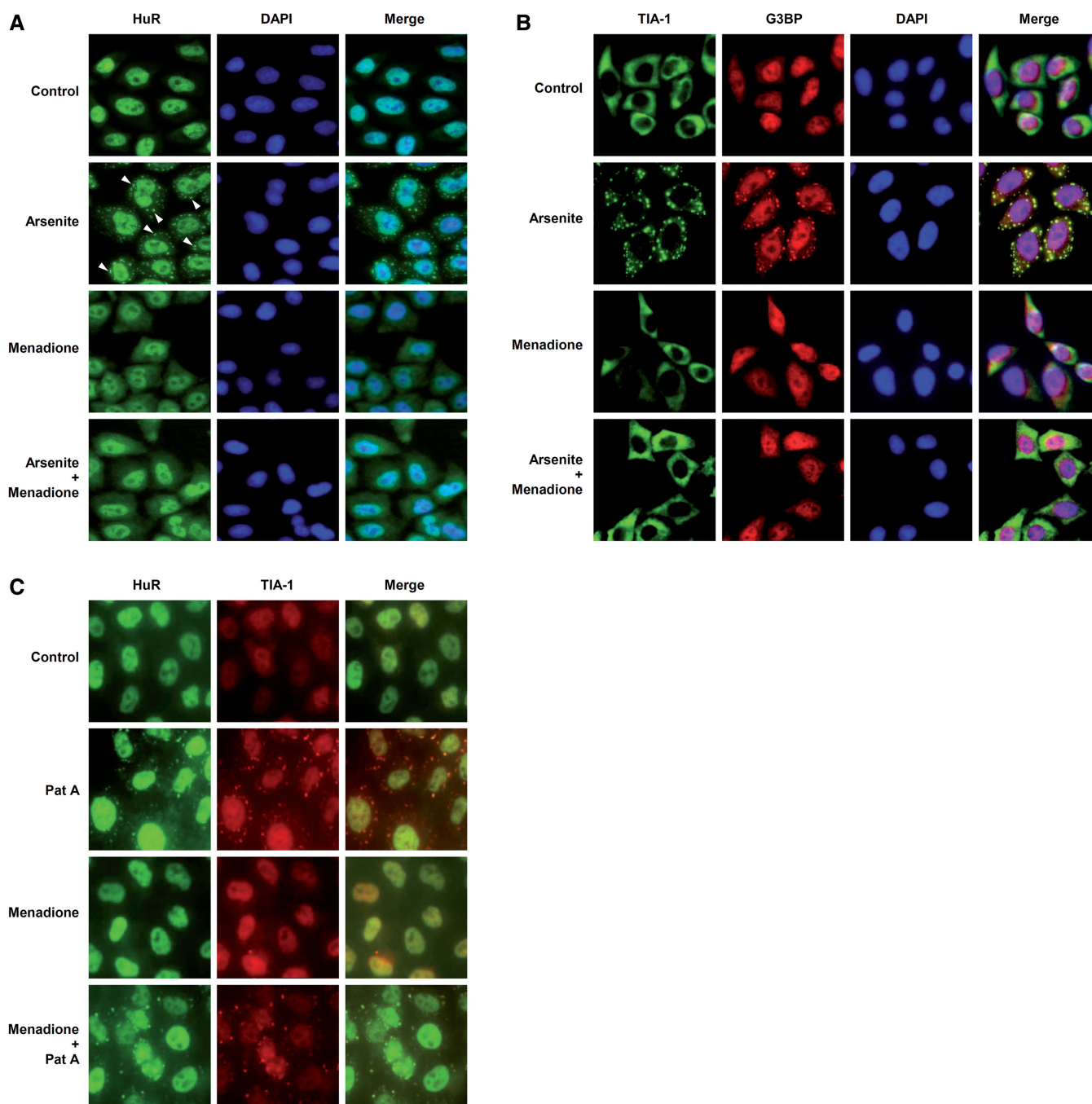
Figure 1. Menadione prevents the accumulation of HuR in arsenite-triggered SGs. (**A**) HeLa cells were treated with sodium arsenite (250 μM) with or without menadione (15 μM) for 45 min, and SGs (arrowheads) were assessed by microscopy. HuR was visualized by immunofluorescence (green), and nuclei were visualized by staining with 4′,6-Diamidino-2-Phenylindole, Dihydrochloride (DAPI) (blue). (**B**) SG markers TIA-1 and G3BP were visualized by immunofluorescence staining (Materials and Methods) in cells treated as explained in (A); nuclei were visualized with DAPI. (**C**) HeLa cells were treated with menadione and/or pateamine A (50 nM), whereupon SG formation was assessed by immunofluorescence.

andB). Because inhibitors are not totally specific, we also tested whether reducing JAK3 levels [achieved by using small interfering (si)RNAs] influenced SG formation after arsenite and menadione treatments. As shown in Figure 2C, 48 h after transfecting JAK3 siRNA in HeLa cells, JAK3 abundance was substantially lower. Importantly, in these cells, menadione treatment no longer blocked arsenite-triggered HuR-containing SGs, whereas in control (Ctrl) siRNA-transfected cells, menadione

continued to block the formation of arsenite-triggered SGs (Figure 2D). In contrast, another stress-activated kinase that can phosphorylate HuR, Chk2, was not found to be implicated in the effects of arsenite and/or menadione (Supplementary Figure S3). The finding that JAK3 silencing mirrored the effect of inhibiting JAK3 lends further support to the notion that activation of JAK3 by menadione prevents the assembly of HuR-containing SGs.
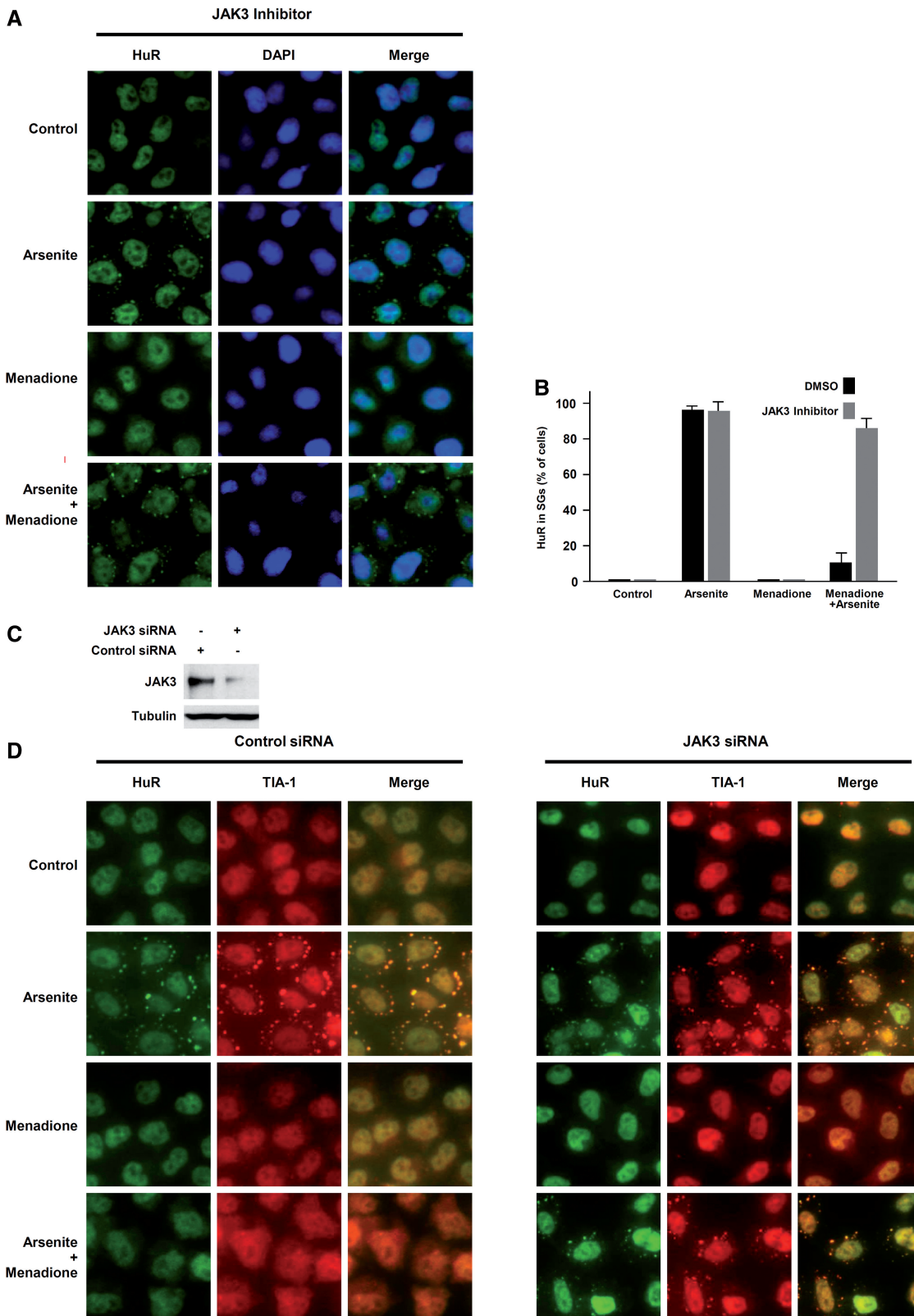
Figure 2. JAK3 inhibits HuR presence in SGs. (**A**) HeLa cells were pre-incubated for 1 h with the JAK3 inhibitor ZM449829 (10 µM) before treatment with arsenite and/or menadione and immunostaining as described in Figure 1A. (**B**) Percentage of HeLa cells with visible SGs (at least one SG per cell) after treatment as in (A); data are the means + SD from three independent experiments. (**C** and **D**) Forty-eight hours after transfection of HeLa cells with either JAK3 or Ctrl siRNAs, the levels of JAK3 (as well as the levels of loading control tubulin) were assessed by WB analysis (C); the formation of SGs was visualized after treating and staining cells as explained in Figure 1D.

The rescue of HuR-positive SGs in HeLa cells after inhibiting JAK3, a tyrosine kinase, raised the intriguing possibility that tyrosine phosphorylation might affect HuR localization in response to arsenite treatment. Even though HuR has not been previously reported to be a tyrosine-phosphorylated protein, we examined whether phosphotyrosine (pY)-HuR was detected in HeLa cells treated with arsenite, with menadione or with both compounds. As shown in Figure 3A, IP of HuR from HeLa cells followed by WB analysis of phosphotyrosine residues using an anti-pY antibody revealed positive pY-HuR signals in menadione-treated cells. To gain further evidence that JAK3 might directly phosphorylate HuR, lysates from HeLa cells that had been treated with arsenite and/or menadione were used to immunoprecipitate JAK3 and recombinant purified MBP-HuR was used as substrate in an *in vitro* kinase assay. This analysis revealed that MBP-HuR was preferentially phosphorylated by JAK3 prepared by IP from menadione-treated cells and further showed that menadione treatment triggered the phosphorylation of JAK3 at residue Y980 (Figure 3B). In addition, IP followed by WB analysis revealed that pY-HuR levels were strongly suppressed in HeLa cells treated with the JAK3 inhibitor ZM 449829 and in HeLa cells in which JAK3 levels were lowered by silencing (Figure 3C). Together, these results indicate that the menadione-activated JAK3 phosphorylates HuR at one or several tyrosines and that this modification is linked to the loss of HuR-positive SGs.

JAK3 phosphorylates HuR at tyrosine residues

To identify the tyrosine residues of HuR that were phosphorylated by JAK3, we performed an *in vitro* kinase assay using recombinant purified JAK3 kinase (Millipore) and MBP-HuR purified from *E. coli* (Figure 3D). Mass spectrometry analysis (Materials and Methods) of the phosphorylated HuR revealed three tyrosines phosphorylated by JAK3: two residing in the RNA-recognition motif 1 (RRM1), Y63 and Y68, and one residing within the hinge region (Y200) surrounding the HNS (Figure 3E).

To investigate the possible impact of these modifications on HuR function, we changed the tyrosines into phenylalanines by site-directed mutagenesis (Y200F, Y68F and Y63F) and expressed the respective point mutants as Flag-HuR proteins from plasmids pFlag-HuR[wild-type (WT)], pFlag-HuR(Y63F), pFlag-HuR(Y68F) and pFlag-HuR(Y200F). Transfection of each plasmid followed by menadione treatment revealed that Flag-HuR(WT) and Flag-HuR(Y63F) were still tyrosine phosphorylated, but Flag-HuR(Y68F) and Flag-HuR(Y200F) were not (Figure 4A), suggesting that menadione elicited phosphorylation of HuR at Y68 and Y200 *in vivo*. It was interesting to note that Y68F and Y200F each completely inhibited phosphorylation, suggesting that perhaps phosphorylation of one of these two tyrosine residues facilitates or is required for phosphorylation of the other tyrosine residue. The basal and menadione-triggered tyrosine phosphorylation of Flag-HuR(WT), Flag-HuR(Y63F), Flag-HuR(Y68F) and

Flag-HuR(Y200F) are shown (Figure 4B). Immuno-fluorescent detection of the Flag tag in cells transfected with these expression plasmids showed that all three Flag-tagged HuR proteins localized to SGs on arsenite treatment (Figure 4C). Interestingly, however, when cells were treated with both arsenite + menadione, Flag-HuR(WT) and Flag-HuR(Y68F) did not localize in visible SGs, whereas Flag-HuR(Y200F) mutant did (Figure 4C). The SG marker TIA-1 colocalized with HuR(Y200F) in SGs of cells treated with arsenite + menadione, supporting the notion that the HuR foci seen under these conditions were *bona fide* SGs (Supplementary Figure S4A). Technical limitations associated with the ability to detect endogenous and ectopic proteins in this experiment precluded a more definitive analysis of SGs (kinetics of assembly/disassembly, size and number) forming in the presence of WT and Y200F mutant HuR. Thus, the extent to which menadione inhibited the recruitment of HuR to SGs or more broadly impaired SG formation could not be determined. However, our results did show that menadione induces the phosphorylation of HuR by JAK3 on tyrosine residues and that phosphorylation at HuR Y200 specifically impacts on HuR subcellular localization.

Phosphorylation at Y200 influences HuR binding to target mRNAs

Because phosphorylation of HuR by other kinases affects HuR binding to target mRNAs, as explained above, we investigated whether phosphorylation by JAK3 influenced HuR binding to target mRNAs. For this, we focused on two well-established HuR target transcripts with abundant expression in HeLa cells, *SIRT1* and *VHL* mRNAs (22,36), encoding the protein deacetylase sirtuin 1 (Sirt1) and the tumor suppressor protein von Hippel-Lindau, respectively. We studied the interaction of HuR with these mRNAs by RIP (ribonucleoprotein immunoprecipitation) analysis of endogenous HuR using an anti-HuR antibody; the efficiency of IP of the endogenous HuR protein was assessed (Supplementary Figure S4B). After isolation of the RNA present in HuR RNP complexes, the levels of specific mRNAs were measured by RT followed by real-time quantitative (q)PCR analysis. As shown (Figure 5A and B), endogenous HuR displayed robust binding to these mRNAs in the absence of additional treatments ('Control' group), but the concentration of these complexes increased strongly after arsenite treatment [and increased even further at higher doses, Supplementary Figure S5]. Following the addition of menadione, with or without arsenite, this heightened interaction was lost and HuR binding to *SIRT1* and *VHL* mRNAs returned to the levels seen in the 'Control' group.

To examine whether HuR phosphorylation at Y200 was involved in these interactions, we transfected plasmids pFlag-HuR(WT), pFlag-HuR(Y68F) and pFlag-HuR(Y200F) and tested the binding of the tagged HuR with *SIRT1* mRNA (*left*) and *VHL* mRNA (*right*) again by RIP analysis, but by using anti-Flag antibody. The efficiency of IP of the Flag-tagged proteins was also monitored (Supplementary Figure S4B). Interestingly, although
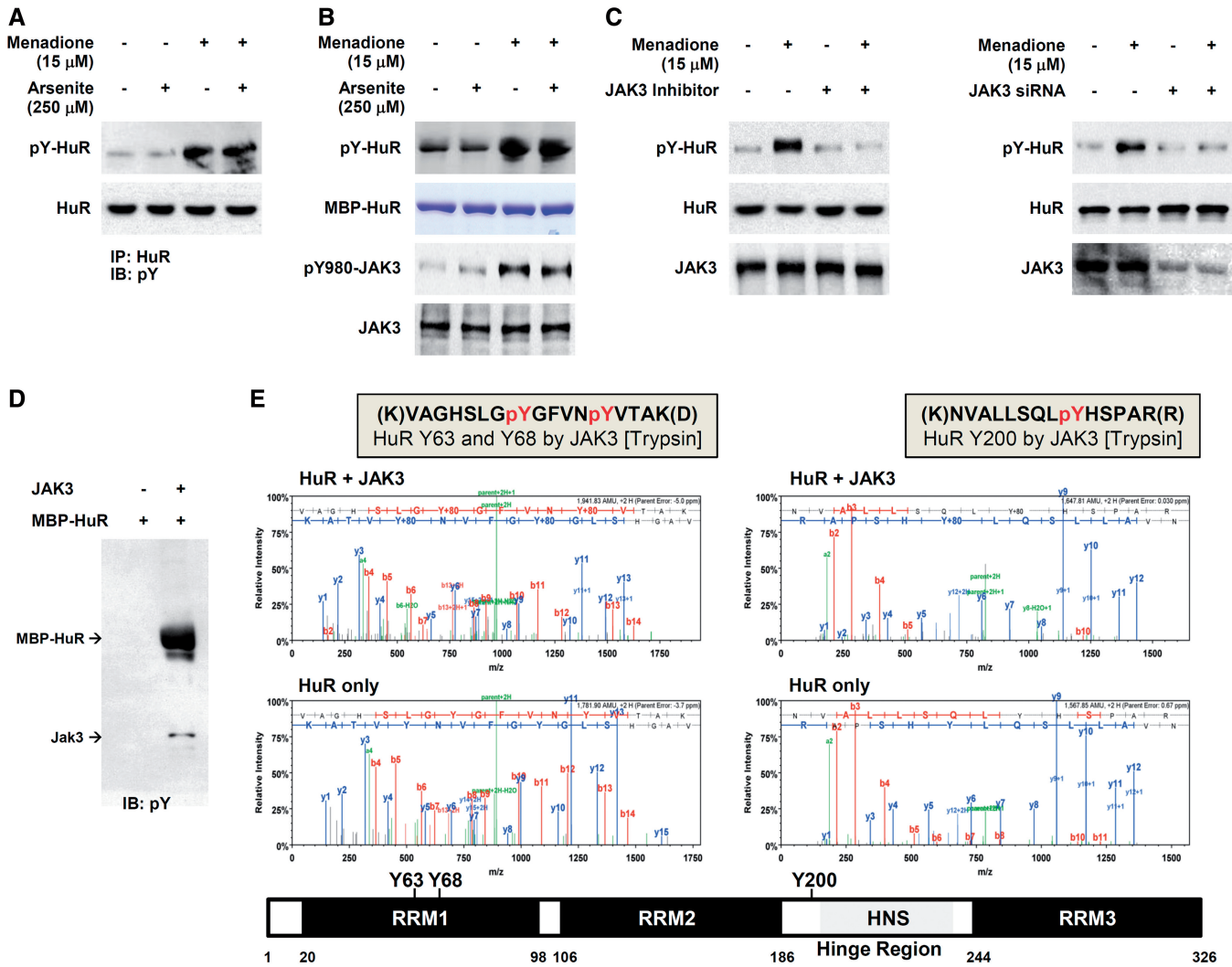
Figure 3. JAK3 phosphorylates HuR at tyrosine residues. (**A**) After treatment with arsenite and/or menadione, HeLa cell lysates were subjected to IP using anti-HuR antibody, and the resulting IP material was assayed by WB analysis using anti-phosphotyrosine (pY) antibody. (**B**) After treatment of cells as in (A), JAK3 was isolated by IP from HeLa cell lysates, and the IP material was used for an *in vitro* kinase assay using recombinant MBP-HuR protein (2 μg) in the presence of ATP; the reaction product was subjected to WB analysis to detect tyrosine-phosphorylated HuR as well as JAK3 phosphorylation at Y980. (**C**) After treatment with menadione and/or JAK3 inhibitor (left), and menadione and/or JAK3 siRNA (right), pY-HuR was detected by IP using anti-HuR antibody and WB using anti-pY antibody. (**D**) Recombinant purified JAK3 kinase (Millipore) was used in *in vitro* kinase assay using recombinant MBP-HuR protein (2 μg) in the presence of ATP; the reaction mixtures were subjected to WB analysis to detect tyrosine-phosphorylated HuR. (**E**) Top: LC–MS/MS analysis to map pY HuR residues phosphorylated by JAK3. MBP-HuR was incubated with or without JAK3 kinase domain (Millipore) in the presence of ATP. The resulting reaction mixtures were digested with trypsin for mass spectrometry analysis. Mass shifts after phosphorylation were shown as Y + 80. Bottom: schematic representation of pY sites on HuR; *RRM*, RNA-recognition motif; *HNS*, HuR nucleocytoplasmic shuttling domain. Data in (A–D) are representative of three independent experiments.

proteins Flag-HuR(WT) and Flag-HuR(Y68F) showed the same pattern of binding as the endogenous HuR, Flag-HuR(Y200F) binding to the mRNAs was no longer repressed after menadione treatment (Figure 5C andD). These results suggest that HuR phosphorylation at Y200 not only prevented HuR localization in SGs, but it also reduced binding of HuR with target *SIRT1* and *VHL* mRNAs.

HuR tyrosine phosphorylation influences target mRNA turnover

Because HuR is known to stabilize *SIRT1* and *VHL* mRNAs (22,36), we examined the effect of HuR tyrosine

phosphorylation on the stability of these target mRNAs. We measured their half-lives by quantifying the rate of decay after transcription was inhibited through the addition of actinomycin D ('Materials and Methods' section). Arsenite treatment, which enhanced HuR binding to these mRNAs, also increased their half-lives (by about twofold; Figure 6A). Menadione alone did not change the stability of target mRNAs, but cells in the menadione + arsenite treatment group showed lower stability for both mRNAs relative to the arsenite alone group (Figure 6A). By contrast, the stability of a control stable transcript, *GAPDH* mRNA, encoding a housekeeping protein, was not influenced by the above-mentioned
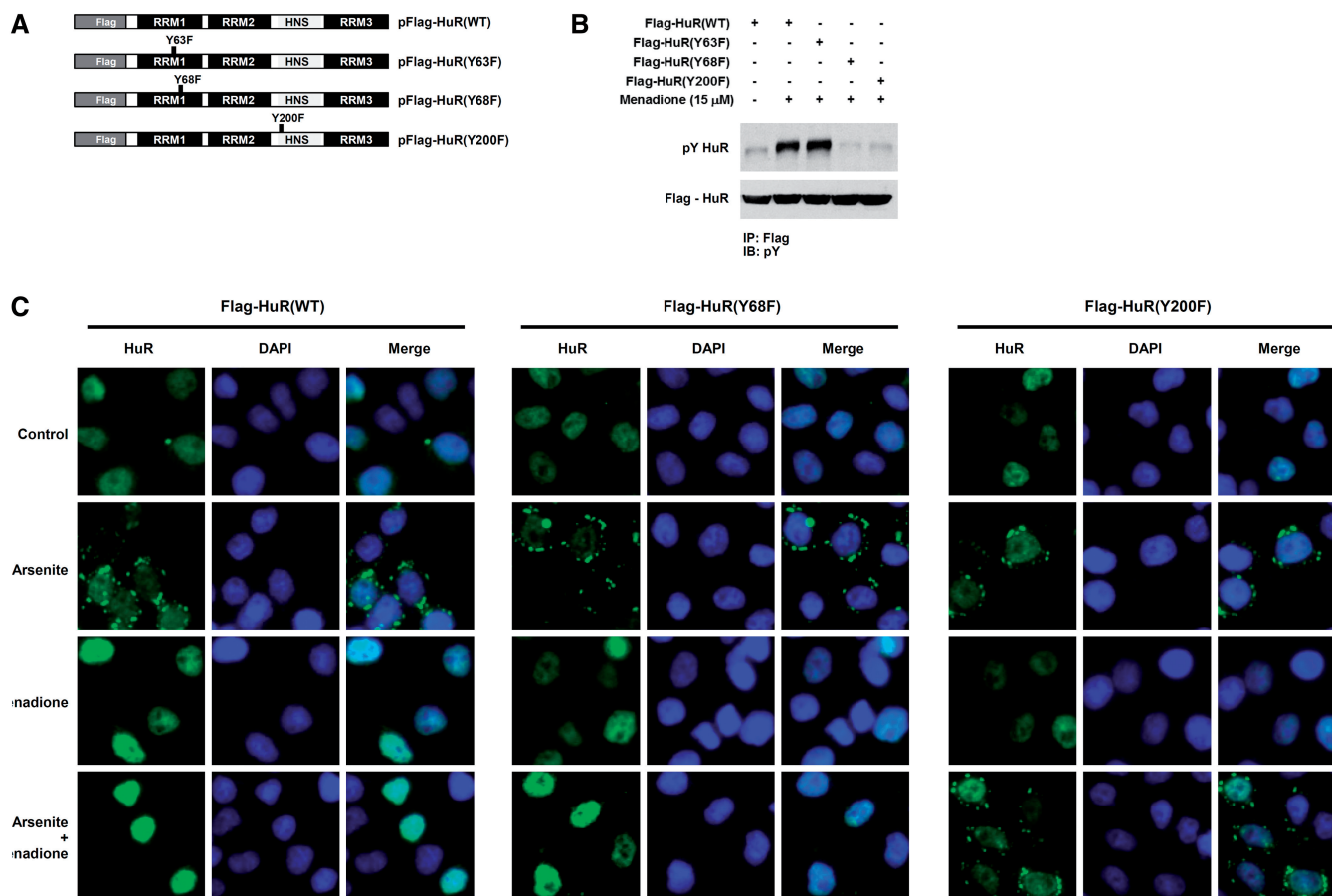
Figure 4. HuR phosphorylation at Y200 blocks its localization in SGs. (**A**) Top: schematic representation of Flag-tagged HuR WT and point mutants Y63F, Y68F and Y200F. (**B**) Forty-eight hours after transfecting HeLa cells with the plasmids shown in (A), cell lysates were prepared, and pY-HuR signals were detected for each Flag-HuR mutant under the conditions shown. (**C**) Plasmids expressing Flag-tagged HuR WT and tyrosine mutants (A) were transfect into HeLa cells; 48 h later, cells were treated with arsenite and/or menadione and distribution of Flag-HuR (WT or point mutants Y68F or Y200F) was characterized using anti-Flag antibody; DAPI staining was included to visualize the nuclei. Data in (A–C) are representative of three independent experiments.

treatments, demonstrating that not all mRNAs decreased rapidly in the presence of actinomycin D, and only select labile mRNAs displayed reduced stability (Figure 6A, bottom). The levels of a control short-lived mRNA (*MYC* mRNA, encoding the proto-oncogene c-Myc) showed reduced half-life in the absence of arsenite (Figure 6A, bottom). These results support the view that HuR binding increases the half-lives of *SIRT1* and *VHL* mRNAs.

Given the documented levels of HuR association with *SIRT1* and *VHL* mRNAs (Figure 5) and the *SIRT1* and *VHL* mRNA half-lives (Figure 6A), we investigated the influence of non-phosphorylatable HuR Y200F mutant on the abundance of these mRNAs. When Flag-HuR(WT) was expressed in HeLa cells, the levels of *SIRT1* and *VHL* mRNAs rose after treatment with arsenite, but this increase was lost if cells were co-treated with menadione (Figure 6B). In contrast, when Flag-HuR(Y200F) was expressed, the arsenite-elicited increase in *SIRT1* mRNA and *VHL* mRNA levels was refractory to menadione treatment, and the mRNAs remained significantly elevated (Figure 6B). In sum, these results indicate that
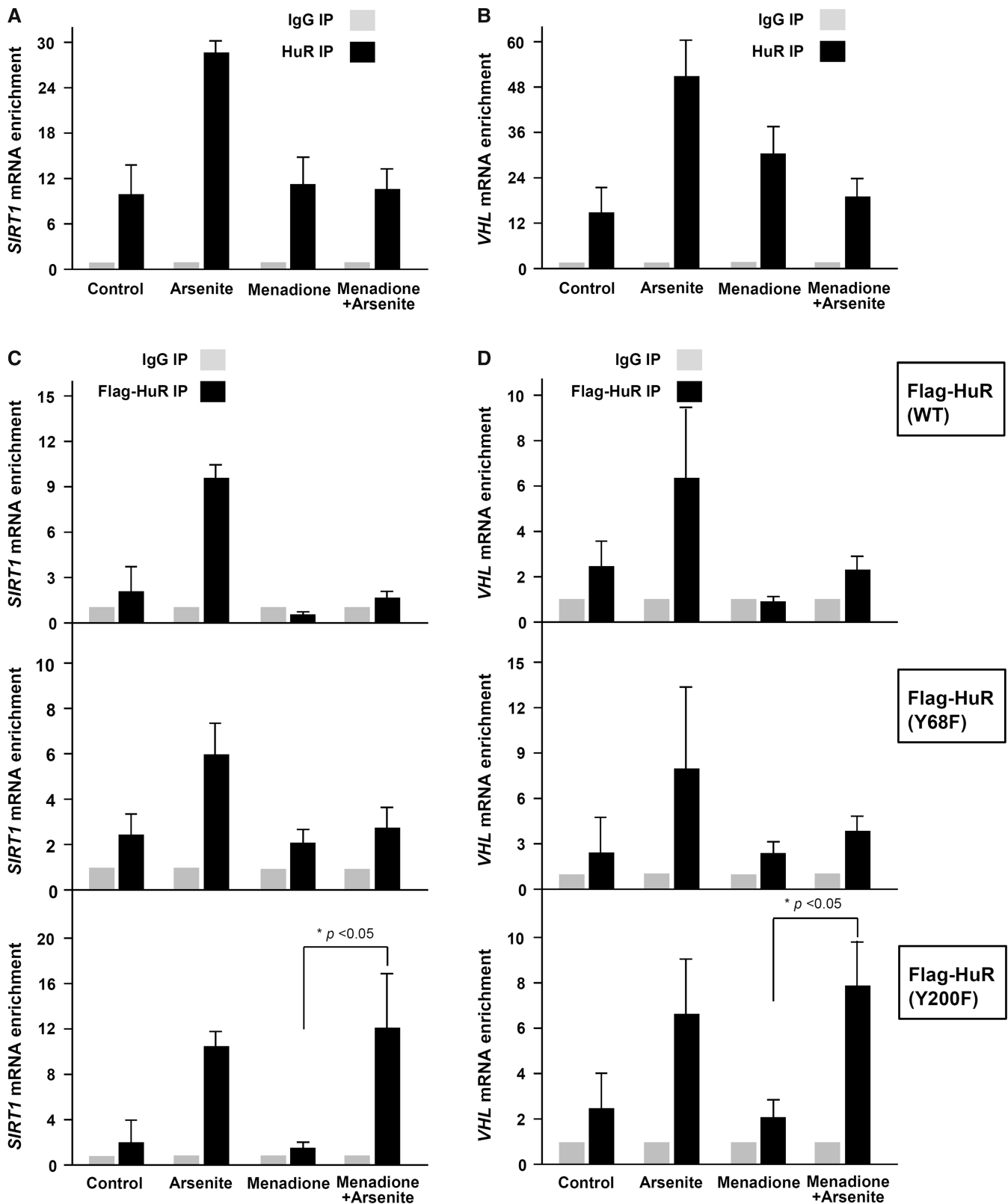
HuR tyrosine phosphorylation at Y200, which excludes HuR from SGs, also promotes the dissociation of HuR from target transcripts (*SIRT1* mRNA and *VHL* mRNA), or perhaps mobilizes HuR-*SIRT1* mRNA and HuR-*VHL* mRNA complexes away from SGs, accelerating their degradation (Figure 7).

DISCUSSION

Tyrosine-phosphorylation of HuR by JAK3

We have reported that tyrosine phosphorylation of HuR reduces its interaction with target mRNAs, leading to lower mRNA stability. The phosphorylation at a tyrosine was unexpected, as earlier work had only identified HuR as the substrate of serine and threonine phosphorylation by PKC, Chk2, p38 and Cdk1 [reviewed in (18)]. In contrast to the earlier phosphorylation events, HuR tyrosine phosphorylation is found to influence mRNA fate linked to the absence of HuR in SGs. JAK3, identified here as a kinase responsible for the tyrosine phosphorylation of HuR, is best known in

Figure 5. Tyrosine phosphorylation of HuR at Y200 reduces its interactions with target mRNAs. (**A, B**) After treatment of HeLa cells with arsenite and/or menadione as explained in Figure 1, RIP (IP followed by RT-qPCR) analysis was used to measure the levels of enrichment of *SIRT1* mRNA (A) and *VHL* mRNA (B) associated with HuR; the samples were normalized using *GAPDH* mRNA, and the data represented as enrichment of each mRNA in HuR IP were compared with IgG IP. (**C, D**) After transfection and treatment, RIP analysis was used to measure the interaction between Flag-HuR (WT, Y68F, Y200F) and *SIRT1* mRNA (C) and *VHL* mRNA (D); *GAPDH* mRNA was measured for normalization, and data are represented as enrichment of the mRNAs in Flag IP samples relative to the levels in IgG IP samples. The graphs represent the means and SD from three independent experiments.
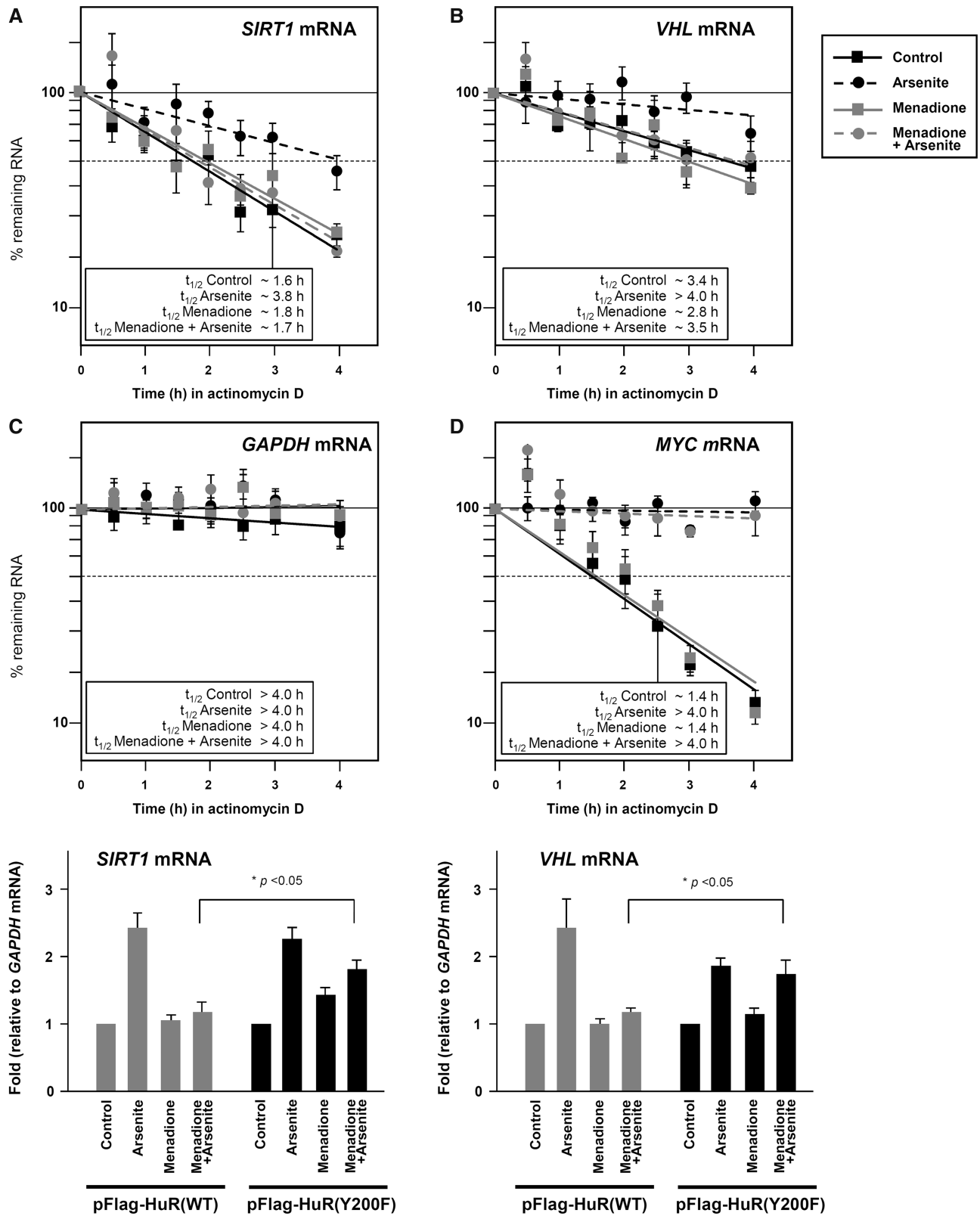
Figure 6. Arsenite and menadione affect the levels and stability of HuR target mRNAs. (**A**) After treatment of arsenite and/or menadione, the half-lives ($t_{1/2}$) of *SIRT1* and *VHL* mRNAs (top), as well as the half-lives of a control stable mRNA (*GAPDH* mRNAs) and a control labile mRNA (*MYC* mRNA) (bottom) were quantified by measuring the time required to achieve a 50% reduction in transcript levels after adding actinomycin D at time 0 h. (**B**) Forty-eight hours after transfecting HeLa cells with plasmids to express Flag-HuR(WT) or Flag-HuR(Y200F), the steady-state levels of *SIRT1* and *VHL* mRNAs were measured by RT-qPCR and normalized to the levels of *GAPDH* mRNA. The graphs represent the means and SD from three independent experiments.
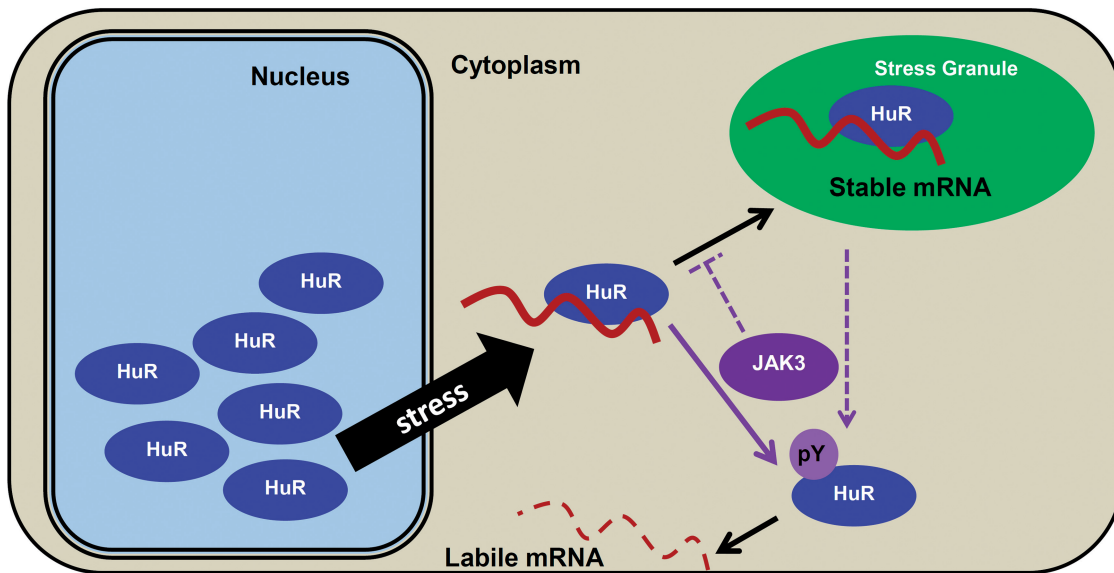
Figure 7. Schematic representation of the proposed influence of JAK3 on HuR localization and RNA-binding activity. See text for details.

immune cells, where it is activated following exposure to cytokines (37). However, JAK3 is also expressed in HeLa cells and its inhibition by ZM 449829 lowers pY-HuR levels. As identified by mass spec analysis, JAK3 phosphorylates three HuR residues (Y63, Y68, Y200), but it remains possible that other tyrosine kinases besides JAK3 can also phosphorylate HuR at tyrosines, although no such kinases have been identified to date. Because the ubiquitous HuR is abundant in immune cells, it will be interesting to test whether tyrosine phosphorylation of HuR at Y200 influences the response of immune cells to cytokines.

Treatment with arsenite or menadione for 45 min caused oxidative stress, and this effect was enhanced by joint treatment with both chemicals (Supplementary Figure S1B). Nonetheless, by 4 h after the drugs were removed from the culture medium, assessments of cell numbers and annexin V-positive cells revealed little or no toxicity (Supplementary Figure S1A, C and D). By 24 h after removing the drugs, cells treated with arsenite did not exhibit much toxicity, as measured by modest cell loss and the absence of annexin V-positive cells (Supplementary Figure S1C and D); however, simultaneous addition of menadione to arsenite-treated cells did prove toxic, as evidenced by the enhanced cell loss and the high percentage of annexin V-positive cells (Supplementary Figure S1C and D). These results indicate that SGs are a component of the stress-response program triggered by arsenite, which ultimately the cells survived. The concomitant treatment with menadione modified this stress-response program (in part by antagonizing the formation of HuR-positive SGs) and potentiated the toxicity of arsenite. It is plausible that the chemotherapeutic actions of menadione (38) are linked to the cytotoxicity caused by menadione, as it interferes with the cellular response to stress conditions.

HNS phosphorylation affects HuR localization and binding to mRNAs

It was somewhat surprising to discover that HuR binding to *SIRT1* and *VHL* mRNAs was influenced by phosphorylation at Y200 (Figure 5), as this residue lies within the shuttling domain of HuR (the HNS) and not within one of the three RRMs. For example, previous reports had shown that phosphorylation at RRMs (S88 in RRM1, T118 in RRM2, S100 between RRM1 and RRM2 and S318 in RRM3) affected HuR binding to numerous mRNAs (18), while phosphorylation in the HNS region (S202, S221, S242), generally altered HuR the relative abundance of HuR in the nucleus compared with the cytoplasm (19–21). The finding that phosphorylation near the shuttling domain affects HuR binding suggests that pY200 could change the conformation of the RRMs in ways that lower their binding affinity for RNA. Alternatively, Y200 phosphorylation could mobilize HuR to areas of the cell that have reduced concentration of HuR target transcripts, and thus binding is reduced because mRNAs are unavailable. Distinguishing between these possibilities awaits further study.

The finding that the non-phosphorylatable HuR(Y200F) is found in SGs after arsenite + menadione, whereas the phosphorylatable counterpart, HuR(WT), is not, suggests that phosphorylation at Y200 actively excludes HuR from SGs. Although the molecular mediators of HuR exclusion from SGs are not identified in our experiments, we have evidence that menadione may block the assembly of other SG components, including TIA-1, G3BP and eIF3b (Figure 1B; Supplementary Figure S6A; data not shown). In fact, it is possible that JAK3 may block the assembly of multiple SG components, perhaps by phosphorylating them in a coordinated manner. In this regard, JAK3 was capable of phosphorylating TIA-1 *in vitro* (Supplementary Figure S6B). Therefore, it

remains formally possible that in cells that form SGs, HuR is mobilized to SGs because the mRNAs that HuR associates with are actively recruited to, or 'pulled to', SGs. It is unknown at present whether JAK3 impairs the binding of HuR to mRNAs and for this reason, HuR is not mobilized to SGs, or instead JAK3 inhibits the mobilization of HuR to SGs and this in turn affects HuR binding to mRNAs locally enriched in SGs. Both possibilities agree with the notion that SGs are sites of mRNA reassortment and 'triage' (30), where mRNA-binding factors form different RNPs to accomplish molecular decisions on mRNA turnover and translational status.

HuR binding to mRNAs increased by stress, linked to stabilization

The discovery that treatment with arsenite, a strong oxidant, increased HuR binding to *SIRT1* and *VHL* mRNAs was also against our expectation (Figure 5A and B; Supplementary Figure S5), as other stress agents (e.g. ionizing radiation and the oxidant hydrogen peroxide) instead triggered the dissociation of HuR from bound mRNAs (22). As dissociation of mRNAs was linked to the phosphorylation of HuR by Chk2, it is possible that arsenite inhibits Chk2 activity, while menadione reverses this inhibition in HeLa cells. Of course, arsenite and/or menadione could also affect the phosphorylation of HuR by other kinases (p38, PKC), which influence HuR–mRNA interactions. Studies are underway to investigate these possibilities, particularly given earlier reports documenting an increase in HuR binding to some mRNAs in response to certain stresses [e.g. *HIF1A* mRNA after hypoxia, *MKP1* mRNA after hydrogen peroxide treatment (39,40)]. In sum, our findings add to a growing body of evidence that underscores the complex regulation of HuR by phosphorylation, and the impact of this modification on HuR localization, HuR binding to mRNAs and the fate of HuR target transcripts.

SUPPLEMENTARY DATA

Supplementary Data are available at NAR Online.

REFERENCES

1. Wilkie,G.S., Dickson,K.S. and Gray,N.K. (2003) Regulation of mRNA translation by 5′- and 3′-UTR-binding factors. *Trends Biochemi. Sci.*, **28**, 182–188.
2. Wilusz,C.J. and Wilusz,J. (2004) Bringing the role of mRNA decay in the control of gene expression into focus. *Trends Genet.*, **20**, 491–497.
3. Moore,M.J. (2005) From birth to death: the complex lives of eukaryotic mRNAs. *Sci. Signal.*, **309**, 1514.
4. Abdelmohsen,K., Kuwano,Y., Kim,H.H. and Gorospe,M. (2008) Posttranscriptional gene regulation by RNA-binding proteins during oxidative stress: implications for cellular senescence. *Biol. Chem.*, **389**, 243–255.
5. Lee,E.K. (2012) Post-translational modifications of RNA-binding proteins and their roles in RNA granules. *Curr. Protein Pept. Sci.*, **13**, 331–336.
6. Srikantan,S. and Gorospe,M. (2008) Regulation of mRNA turnover by cellular stress. In: Bradshaw,R.A. and Dennis,E.A. (eds), *Handbook of Cell Signaling*, Chapter 270.
7. Izquierdo,J.M. (2008) Hu antigen R (HuR) functions as an alternative pre-mRNA splicing regulator of Fas apoptosis, promoting receptor on exon definition. *J. Biol. Chem.*, **283**, 19077–19084.
8. Wang,H., Molfenter,J., Zhu,H. and Lou,H. (2010) Promotion of exon 6 inclusion in HuD pre-mRNA by Hu protein family members. *Nucleic Acids Res.*, **38**, 3760–3770.
9. Mukherjee,N., Corcoran,D.L., Nusbaum,J.D., Reid,D.W., Georgiev,S., Hafner,M., Ascano,M. Jr, Tuschl,T., Ohler,U. and Keene,J.D. (2011) Integrative regulatory mapping indicates that the RNA-binding protein HuR couples pre-mRNA processing and mRNA stability. *Mol. Cell*, **43**, 327–339.
10. López de Silanes,I., Zhan,M., Lal,A., Yang,X. and Gorospe,M. (2004) Identification of a target RNA motif for RNA-binding protein HuR. *Proc. Natl Acad. Sci. USA*, **101**, 2987–2992.
11. Brennan,C.M. and Steitz,J.A. (2001) HuR and mRNA stability. *Cell. Mol. Life Sci.*, **58**, 266–277.
12. Abdelmohsen,K. and Gorospe,M. (2010) Posttranscriptional regulation of cancer traits by HuR. *Wiley Interdiscip. Rev. RNA*, **1**, 214–229.
13. Srikantan,S. and Gorospe,M. (2012) HuR function in disease. *Front. Biosci.*, **17**, 189–205.
14. Gallouzi,I.E. and Steitz,J.A. (2001) Delineation of mRNA export pathways by the use of cell-permeable peptides. *Science*, **294**, 1895–1901.
15. Fan,X.C. and Steitz,J.A. (1998) HNS, a nuclearcytoplasmic shuttling sequence in HuR. *Proc. Natl Acad. Sci. USA*, **95**, 15293–15298.
16. Güttinger,S., Mühlhäusser,P., Koller-Eichhorn,R., Brennecke,J. and Kutay,U. (2004) Transportin2 functions as importin and mediates nuclear import of HuR. *Proc. Natl Acad. Sci. USA*, **101**, 2918–2923.
17. Rebane,A., Aab,A. and Steitz,J.A. (2004) Transportins 1 and 2 are redundant nuclear import factors for hnRNP A1 and HuR. *RNA*, **10**, 590–599.
18. Eberhardt,W., Doller,A. and Pfeilschifter,J. (2012) Regulation of the mRNA-binding protein HuR by posttranslational modification: spotlight on phosphorylation. *Curr. Protein Pept. Sci.*, **13**, 380–390.
19. Kim,H.H., Abdelmohsen,K., Lal,A., Pullmann,R. Jr, Yang,X., Galban,S., Srikantan,S., Martindale,J.L., Blethrow,J., Shokat,K.M. *et al.* (2008) Nuclear HuR accumulation through phosphorylation by Cdk1. *Genes Dev.*, **22**, 1804–1815.
20. Kim,H.H., Yang,X., Kuwano,Y. and Gorospe,M. (2008) Modification at HuR(S242) alters HuR localization and proliferative influence. *Cell Cycle*, **7**, 3371–3377.
21. Kim,H.H. and Gorospe,M. (2008) Phosphorylated HuR shuttles in cycles. *Cell Cycle*, **7**, 3124–3126.
22. Abdelmohsen,K., Pullmann,R. Jr, Lal,A., Kim,H.H., Galban,S., Yang,X., Blethrow,J.D., Walker,M., Shubert,J., Gillespie,D.A. *et al.* (2007) Phosphorylation of HuR by Chk2 regulates SIRT1 expression. *Mol. Cell*, **25**, 543–557.
23. Masuda,K., Abdelmohsen,K., Kim,M.M., Srikantan,S., Lee,E.K., Tominaga,K., Selimyan,R., Martindale,J.L., Yang,X.,

Lehrmann,E. *et al.* (2011) Global dissociation of HuR-mRNA complexes promotes cell survival after ionizing radiation. *EMBO J.*, **30**, 1040–1053.

24. Piecyk,M., Wax,S., Beck,A.R., Kedersha,N., Gupta,M., Maritim,B., Chen,S., Gueydan,C., Kruys,V., Streuli,M. *et al.* (2000) TIA-1 is a translational silencer that selectively regulates the expression of TNF-α. *EMBO J.*, **19**, 4154–4163.

25. Hinman,M.N. and Lou,H. (2008) Diverse molecular functions of Hu proteins. *Cell Mol. Life Sci.*, **65**, 3168–3181.

26. Lian,X.J. and Gallouzi,I.E. (2009) Oxidative stress increases the number of stress granules in senescent cells and triggers a rapid decrease in p21waf1/cip1 translation. *J. Biol. Chem.*, **284**, 8877–8887.

27. Lu,L., Wang,S., Zheng,L., Li,X., Suswam,E.A., Zhang,X., Wheeler,C.G., Nabors,L.B., Filippova,N. and King,P.H. (2009) Amyotrophic lateral sclerosis-linked mutant SOD1 sequesters Hu antigen R (HuR) and TIA-1-related protein (TIAR): implications for impaired post-transcriptional regulation of vascular endothelial growth factor. *J. Biol. Chem.*, **284**, 33989–33998.

28. Bhattacharyya,S.N., Habermacher,R., Martine,U., Closs,E.I. and Filipowicz,W. (2006) Relief of microRNA-mediated translational repression in human cells subjected to stress. *Cell*, **125**, 1111–1124.

29. Stoecklin,G., Stubbs,T., Kedersha,N., Wax,S., Rigby,W.F., Blackwell,T.K. and Anderson,P. (2004) MK2-induced tristetraprolin:14-3-3 complexes prevent stress granule association and ARE-mRNA decay. *EMBO J.*, **23**, 1313–1324.

30. Anderson,P. and Kedersha,N. (2009) RNA granules: post-transcriptional and epigenetic modulators of gene expression. *Nat. Rev. Mol. Cell Biol.*, **10**, 430–436.

31. Yoon,J.H., Choi,E.J. and Parker,R. (2010) Dcp2 phosphorylation by Ste20 modulates stress granule assembly and mRNA decay in *Saccharomyces cerevisiae*. *J. Cell Biol.*, **189**, 813–827.

32. Wiśniewski,J.R., Zougman,A., Nagaraj,N. and Mann,M. (2009) Universal sample preparation method for proteome analysis. *Nat. Methods.*, **6**, 359–362.

33. Kedersha,N., Chen,S., Gilks,N., Li,W., Miller,I.J., Stahl,J. and Anderson,P. (2002) Evidence that ternary complex (eIF2-GTP-tRNA(i)(Met))-deficient preinitiation complexes are core constituents of mammalian stress granules. *Mol. Biol. Cell*, **13**, 195–210.

34. Dang,Y., Kedersha,N., Low,W.K., Romo,D., Gorospe,M., Kaufman,R., Anderson,P. and Liu,J.O. (2006) Eukaryotic initiation factor 2alpha-independent pathway of stress granule induction by the natural product pateamine A. *J. Biol. Chem.*, **281**, 32870–32878.

35. Abdelmohsen,K., Srikantan,S., Tominaga,K., Kang,M.J., Yaniv,Y., Martindale,J.L., Yang,X., Park,S.S., Becker,K.G., Subramanian,M. *et al.* (2012) Growth inhibition by miR-519 via multiple p21-inducing pathways. *Mol. Cell. Biol.*, **32**, 2530–2548.

36. Abdelmohsen,K., Srikantan,S., Yang,X., Lal,A., Kim,H.H., Kuwano,Y., Galban,S., Becker,K.G., Kamara,D., de Cabo,R. *et al.* (2009) Ubiquitin-mediated proteolysis of HuR by heat shock. *EMBO J.*, **28**, 1271–1282.

37. O'Shea,J.J., Holland,S.M. and Staudt,L.M. (2013) JAKs and STATs in immunity, immunodeficiency, and cancer. *N. Engl. J. Med.*, **368**, 161–170.

38. Nutter,L.M., Cheng,A.L., Hung,H.L., Hsieh,R.K., Ngo,E.O. and Liu,T.W. (1991) Menadione: spectrum of anticancer activity and effects on nucleotide metabolism in human neoplastic cell lines. *Biochem. Pharmacol.*, **41**, 1283–1292.

39. Galbán,S., Kuwano,Y., Pullmann,R. Jr, Martindale,J.L., Kim,H.H., Lal,A., Abdelmohsen,K., Yang,X., Dang,Y., Liu,J.O. *et al.* (2008) RNA-binding proteins HuR and PTB promote the translation of hypoxia-inducible factor 1α. *Mol. Cell. Biol.*, **28**, 93–107.

40. Kuwano,Y., Kuwano,Y., Pullmann,R. Jr, Martindale,J.L., Kim,H.H., Lal,A., Abdelmohsen,K., Yang,X., Dang,Y., Liu,J.O. *et al.* (2008) MKP-1 mRNA stabilization and translational control by RNA-binding proteins HuR and NF90. *Mol. Cell. Biol.*, **28**, 4562–4575.